EFFECTS OF ARYL HYDROCARBON RECEPTOR LIGAND TCDD ON HUMAN TROPHOBLAST CELL DEVELOPMENT

Vinay Shukla[a,b,1,2], Khursheed Iqbal[a,b,3], Hiroaki Okae[c], Takahiro Arima[d], and Michael J. Soares[a,b,e,f,1]

[a]Institute for Reproductive and Developmental Sciences, University of Kansas Medical Center, Kansas City, KS 66160

[b]Department of Pathology and Laboratory Medicine, University of Kansas Medical Center, Kansas City, KS 661602

[c]Department of Trophoblast Research, Institute of Molecular Embryology and Genetics, Kumamoto University, Kumamoto 860-0811 Japan

[d]Department of Informative Genetics, Environment and Genome Research Center, Tohoku University Graduate School of Medicine, Sendai 980-8575, Japan

[e]Center for Perinatal Research, Children's Mercy Research Institute, Children's Mercy, Kansas City, MO 64108

[f]Department of Obstetrics and Gynecology, University of Kansas Medical Center, Kansas City, KS 66160

[1]**Correspondence:** vshukla@som.umaryland.edu or msoares@kumc.edu

[2]**Current address:** Department of Obstetrics, Gynecology and Reproductive Sciences, University of Maryland School of Medicine, Baltimore, MD

[3]**Current address:** Department of Animal and Food Sciences, Oklahoma State University, Stillwater, OK

The authors declare they have no actual or potential competing financial interests.

Author contributions: V.S. and M.J.S. designed research; V.S. performed research; V.S., K.I., H.O., and T.A. contributed new reagents/analytic tools; V.S., K.I., and M.J.S. analyzed data; V.S. and M.J.S. prepared the manuscript; All authors contributed to editing the manuscript.

Running title: AHR activation and trophoblast cell development

***Key Words*: Placenta, AHR, TCDD, trophoblast cells**

ABSTRACT

BACKGROUND: The primary interface between mother and fetus, the placenta, serves two critical functions: extraction of nutrients from the maternal compartment and facilitation of nutrient delivery to the developing fetus. This delivery system also serves as a barrier to environmental exposures. The aryl hydrocarbon receptor (**AHR**) is an important component of the barrier. AHR signaling is activated by environmental pollutants and toxicants that can potentially affect cellular and molecular processes, including those controlling trophoblast cell development and function.

OBJECTIVES: In this study, we investigated the impact of 2,3,7,8-tetrachlorodibenzo-p-dioxin (**TCDD**), an effective AHR ligand, exposure on human trophoblast cells.

METHODS: Human trophoblast stem (**TS**) cells were used as in vitro model system for investigating the downstream consequences of AHR activation. The actions TCDD were investigated in human TS cells maintained in the stem state or in differentiating TS cells.

RESULTS: TCDD exposure stimulated the expression of *CYP1A1* and *CYP1B1* in human TS cells. TCDD was effective in stimulating *CYP1A1* and *CYP1B1* expression and altering gene expression profiles in human TS cells maintained in the stem cell state or induced to differentiate into extravillous trophoblast cells (**EVT**) or syncytiotrophoblast (**ST**). These actions were dependent upon the presence of AHR. TCDD exposure did not adversely affect maintenance of the TS cell stem state or the ability of TS cells to differentiate into EVT cells or ST. However, TCDD exposure did promote the biosynthesis of 2 methoxy estradiol (**2ME**), a biologically active catechol estrogen, with the potential to modify the maternal-fetal interface.

DISCUSSION: Human trophoblast cell responses to TCDD were dependent upon AHR signaling and possessed the potential to shape development and function of the human placentation site.

INTRODUCTION

The placenta is a specialized organ that enables a safe and supportive environment for the fetus to develop within the female reproductive tract. Functional properties of the placenta are attributed to specialized lineages of trophoblast cells (**Soares et al. 2018; Knofler et al. 2019**). Disruptions in trophoblast cell differentiation and placental morphogenesis affect fetal development and contribute to the origins of adult disease (**Burton et al. 2016**). There is a myriad of environmental exposures that could impact placentation and embryonic development (**Mattison 2010; Marsit 2016; Vrooman and Bartolomei 2016**). An environmental exposure may lead to placental dysmorphogenesis and dysfunction and/or may exacerbate placental dysfunction in pregnancy-associated diseases. Timing of environmental exposures is likely critical in determining their effects on placentation and postnatal health (**Barouki et al. 2012**). The impact of environmental exposures on placental development has received limited experimental attention.

Some environmental toxicants affect cellular function through physical interactions with the aryl hydrocarbon receptor (**AHR**) (**Beisclag et al. 2008; McIntosh et al. 2010; Avilla et al. 2020**). These compounds are effectively ligands for AHR and include halogenated aromatic hydrocarbons (e.g. polychlorinated biphenyls, polychlorinated dibenzodioxins, and dibenzofurans), polycyclic aromatic hydrocarbons (e.g. benzo[a]pyrene and benzanthracene), indoles, flavones, benzoflavones, imidazoles, pyridines, lipids, and lipid metabolites (**Birnbaum 1994; DeGroot et al. 2012; Murray and Perdue 2020**). AHR is a ligand-activated transcription factor and member of the PER–ARNT–SIM subgroup of the basic helix-loop-helix superfamily of transcription factors (**Vazquez-Rivera et al. 2021**). Upon ligand binding, AHR translocates to

the nucleus and heterodimerizes with AHR nuclear translocator (**ARNT**) (**Beisclag et al. 2008; McIntosh et al. 2010**). This heterodimer binds to aryl hydrocarbon response elements (**AHREs**) located within regulatory regions of target genes, including those encoding proteins that are important in biotransformation, drug metabolism, and detoxification of environmental pollutants (**Beisclag et al. 2008; McIntosh et al. 2010; Avilla et al. 2020**). Cytochrome P450 family 1 subfamily A member 1 (**CYP1A1**) is a prototypical transcriptionally activated gene induced by AHR signaling (**Whitlock 1999; Ma 2001**). AHR has been implicated as a regulator of a wide range of biological processes critical for embryonic development and homeostasis (**Zablon et al. 2021**).

The barrier for progress in understanding the impact of environmental exposures on placental development is the implementation of appropriate experimental models to test relevant hypotheses. In vitro approaches are powerful. There are wide range of immortalized and transformed cell models that have been used with the goal of elucidating trophoblast cell responses to AHR ligands (**Zhang et al. 1995, 1997, 1998; Stejskalova et al. 2011, 2013; Tsang et al. 2012; Fadiel et al. 2013; Le Vee et al. 2014; Wu et al. 2016; Dral et al. 2019**). Unfortunately, deciphering trophoblast cell biology using immortalized and transformed cell models is inherently confounding with questionable relevance (**Lee et al. 2016**). The isolation and culture of trophoblast stem (**TS**) cells from several species, including rodents and primates, represented a major advance for investigating trophoblast cell lineage development (**Tanaka et al. 1998; Asanoma et al. 2011; Okae et al. 2018; Matsumoto et al. 2020; Schmidt et al. 2020**).

In this proposal, we investigated an environmental exposure, 2,3,7,8-tetrachlorodibenzo-p-dioxin (**TCDD**), that is a known activator of AHR signaling, and its impact on trophoblast cell development using human TS cells. TCDD exposure modulated the developmental fates of human TS cells.

METHODS

Chemicals

2,3,7,8-tetrachlorodibenzo-p-dioxin (**TCDD**, D-404S) was obtained from AccuStandard and solubilized in dimethyl sulfoxide (**DMSO**, D8418, Sigma-Aldrich). 17β estradiol was purchased from Sigma-Aldrich (3301) and solubilized in ethanol.

Human TS Cell Culture

Cytotrophoblast-derived human TS cell lines (CT27, 46, X,X; CT29, 46, X,Y) were maintained in the stem state or differentiated into extravillous trophoblast (**EVT**) cells or syncytiotrophoblast (**ST**), as described previously (**Okae et al. 2018**). Human TS cells were routinely cultured in 100 mm tissue culture dishes coated with 5 μg/mL of mouse collagen IV (35623, Discovery Labware) or human collagen IV (5022, Advanced Biomatrix). Complete TS Cell Medium was used to maintain cells in the stem state and consisted of Basal TS Cell Medium [DMEM/F12 (11320033, Thermo Fisher), 100 μm 2-mercaptoethanol, 0.2% (vol/vol) fetal bovine serum (**FBS**), 50 μM penicillin, 50 U/mL streptomycin, 0.3% bovine serum albumin (**BSA**, BP9704100, Thermo Fisher), 1% insulin-transferrin-selenium-ethanolamine solution (vol/vol, Thermo-Fisher)] with the addition of 200 μM L-ascorbic acid (A8960, Sigma-Aldrich), 50 ng/mL of epidermal growth factor (**EGF**, E9644, Sigma-Aldrich), 2 μM CHIR99021 (04-

0004, Reprocell), 0.5 μM A83-01 (04-0014, Reprocell), 1 μM SB431542 (04-0010, Reprocell), 0.8 mM valproic acid (P4543, Sigma-Aldrich), and 5 μM Y27632 (04-0012-02, Reprocell).

EVT cell differentiation. To promote EVT cell differentiation, human TS cells were cultured in 6-well plates pre-coated with 1 μg/mL of collagen IV at a density of 80,000 cells per well. Cells were cultured in EVT Cell Differentiation Medium, which consists of the Basal TS Cell Medium with the addition of 100 ng/mL of neuregulin 1 (**NRG1**, 5218SC, Cell Signaling), 7.5 μM A83-01, 2.5 μM Y27632, 4% KnockOut Serum Replacement (**KSR**, 10828028, Thermo Fisher), and 2% Matrigel (CB-40234, Thermo Fisher) (**Okae et al. 2018**). On day 3 of differentiation, the medium was replaced with EVT Differentiation Medium excluding NRG1 and with a reduced Matrigel concentration of 0.5%. On culture day 6 of EVT cell differentiation, the medium was replaced with EVT Differentiation Medium excluding NRG1 and KSR, and with a Matrigel concentration of 0.5%. Cells were analyzed on day 8 of EVT cell differentiation.

ST differentiation. To promote ST differentiation, TS cells were cultured in 6-well plates at a density of 300,000 cells per well using ST-Three Dimensional (**ST3D**) Medium, which consists of Basal TS Cell Medium with a decreased concentration of BSA (0.15%) and the addition of 200 μM L-ascorbic acid, 5% KSR, 2.5 μM Y27632), 2 μM forskolin (F6886, Sigma-Aldrich), and 50 ng/mL of EGF (**Okae et al. 2018**). On day 3 of cell differentiation, 3 mL of fresh ST3D Medium was added to the wells. Cells were analyzed on day 6 of ST differentiation.

Flow cytometry assay for cell death measurement

Cells (2×10^5 cells/ml) were cultured in 6-well plates and expose with TCDD (10 nM and 100 nM) for 24 h. Cells were trypsinized, washed with PBS and probed with FITC-conjugated Annexin-V and PI for 15 min. The staining profiles were determined flow cytometry.

Cell cycle analysis

Cells (2×10^5 cells/ml) were cultured in 6-well plates and expose with TCDD (10 nM and 100 nM) for 24 h. Cells were trypsinized, washed with PBS, fixed in 70% ice-cold ethanol at 4 °C overnight, washed with PBS again, and stained with 200 µl of 50 mg/l propidium iodide at 37 °C for 20 min. Cell cycle distribution was determined by measuring the cellular DNA content with the use of flow cytometry.

Immunofluorescence

Human TS cells in the stem state or differentiated EVT cells were fixed with 4% paraformaldehyde (Sigma-Aldrich) for 20 min at room temperature. Immunofluorescence analysis was performed using a primary antibody against CYP1A1 (1:500, A3001; XenoTech) or AHR (1:500, MA1-514, Thermo Fisher). Alexa Fluor 488 goat anti-mouse IgG (1:800, A32723 Thermo Fisher), Alexa Fluor 568 goat anti-mouse IgG (1:800, A11031, Thermo Fisher), Alexa Fluor 568 goat anti-rabbit IgG, (1:800, A10042, Thermo Fisher) were used to detect locations of the primary antibody-antigen complexes within cells. Nuclei were visualized by staining with 4'6'-diamidino-2-phenylindole (**DAPI**, Molecular Probes). Images were captured on a Nikon 90i upright microscope with a Roper Photometrics CoolSNAP-ES monochrome camera.

Short Hairpin RNA (shRNA) Constructs and Lentivirus Production

AHR shRNAs were subcloned into the pLKO.1 vector at *AgeI* and *EcoRI* restriction sites. shRNA sequences used in the analyses are provided in **Table S1**. Lentiviral packaging vectors

were obtained from Addgene and included pMDLg/pRRE (plasmid 12251), pRSVRev (plasmid 12253), and pMD2.G (plasmid 12259). Lentiviral particles were produced following transient transfection of the shRNA-pLKO.1 vector and packaging plasmids into Lenti-X cells (632180, Takara Bio USA) using Attractene (301005, Qiagen) in Opti-MEM I (51985-034, Thermo Fisher). Cells were maintained in DMEM culture medium (11995-065, Thermo Fisher) supplemented with 10% FBS until 24 h prior to supernatant collection, at which time the cells were cultured in Basal TS Cell Medium supplemented with 200 μM L-ascorbic acid and 50 ng/mL of EGF.

Lentiviral Transduction

Human TS cells were plated at 80,000 cells per well in 6-well tissue culture plates coated with 5 μg/mL collagen IV and incubated for 24 h. Immediately prior to transduction, medium was changed, and cells were incubated with 2.5 μg/mL polybrene for 30 min at 37°C. Immediately following polybrene incubation, TS cells were transduced with 500 μL of lentiviral supernatant and then incubated for 24 h. Medium was changed at 24 h post-transduction and selected with puromycin dihydrochloride (5 μg/mL, A11138-03, Thermo Fisher) for two days. Surviving cells were cultured for one to three days in Complete Human TS Culture Medium before passaging and initiating EVT cell or ST differentiation.

RNA Isolation, cDNA Synthesis, and Reverse Transcriptase-quantitative Polymerase Chain Reaction (RT-qPCR)

Total RNA was isolated from cells and tissues with TRIzol reagent (15596018, Thermo Fisher). cDNA was synthesized from 1 μg of total RNA using a High-Capacity cDNA Reverse

Transcription kit (4368813; Thermo Fisher) and diluted 10 times with water. RT-qPCR was performed using a reaction mixture containing PowerSYBR Green PCR Master Mix (4367659; Thermo Fisher) and primers (250 nM each). PCR primer sequences are presented in **Table S2**. Amplification and fluorescence detection were carried out using a QuantStudio 7 Flex Real-Time PCR System (Thermo Fisher). An initial step (95 °C, 10 min) preceded by 40 cycles of a two-step PCR at: 92 °C, for 15 s and 60 °C for 1 min, followed by a dissociation step (95 °C for 15 s, 60 °C for 15 s, and 95 °C for 15 s). The comparative cycle threshold method was used for relative quantification of mRNA normalized to a housekeeping transcript, glyceraldehyde-3-phosphate dehydrogenase (*GAPDH*).

RNA Sequencing (RNA-seq) Analysis

Transcript profiles were generated from human TS cells cultured in various differentiation states under control conditions or in the presence of AHR ligands (n=3/condition). Complementary DNA libraries from total RNA samples were prepared with Illumina TruSeq RNA preparation kits (RS-122-2101, Illumina) according to the manufacturer's instructions. RNA integrity was assessed using an Agilent 2100 Bioanalyzer (Agilent Technologies). Barcoded cDNA libraries were multiplexed onto a TruSeq paired-end flow cell and sequenced (100-bp paired-end reads) with a TruSeq 200-cycle SBS kit (Illumina). Libraries were sequenced on Illumina HiSeq 2000 sequencer or Illumina NovaSeq 6000 at the University of Kansas Medical Center (**KUMC**) Genome Sequencing Facility. Reads from *.fastq files were mapped to the human reference genome (GRCh37) using CLC Genomics Workbench 12.0 (Qiagen). Transcript abundance was expressed as reads per kilobase of transcript per million mapped reads (**RPKM**), and a false discovery rate of 0.05 was used as a cutoff for significant differential

expression. Statistical significance was calculated by empirical analysis of digital gene expression followed by Bonferroni's correction. Functional patterns of transcript expression were further analyzed using Ingenuity Pathway Analysis (Qiagen).

Measurement of 2-Methoxyestradiol (2ME)

Conditioned medium from TS cells maintained in the stem state and following differentiation were collected and 2ME measured using an enzyme-linked immunosorbent assay (**ELISA**, 582261, Cayman Chemical).

Western Blot Analysis

Cell lysates were prepared by sonication in radioimmunoprecipitation assay lysis buffer (sc-24948A, Santa Cruz Biotech) supplemented with Halt protease and a phosphatase inhibitor mixture (78443, Thermo Fisher). Protein concentrations were measured using the DC Protein Assay (5000113-115, Bio-Rad). Proteins (20 μg/lane) were separated by sodium dodecyl sulfate polyacrylamide gel electrophoresis and transferred onto polyvinylidene difluoride membranes (10600023, GE Healthcare). After transfer, membranes were blocked with 5% non-fat milk in Tris buffered saline with 0.1% Tween 20 (**TBST**) and probed with primary antibodies to AHR (1:1000 dilution, MA1-514, Thermo Fisher) or GAPDH (1:1000 dilution, ab9485, Abcam) overnight at 4°C. Membranes were washed three times for five min with TBST and then incubated with secondary antibodies (goat anti-rabbit IgG HRP, A0545; Sigma-Aldrich and goat anti-mouse IgG HRP, 7076; Cell Signaling) for 1 h at room temperature. Immunoreactive proteins were visualized by enhanced chemiluminescence (Amersham).

Statistical Analysis

Statistical analyses were performed with GraphPad Prism 9 software. Welch's *t* tests, Brown–Forsythe and Welch analysis of variance (**ANOVA**) were applied as appropriate. Statistical significance was determined as $P<0.05$.

RESULTS

Examination of the effects of TCDD exposure on human trophoblast cells

We examined the effects of TCDD in human TS cells at three developmental states: i) stem cell state, ii) EVT cell differentiation state, and iii) ST differentiation state.

Stem cell state. Human TS cells can expand and exhibit a signature transcript profile when maintained in a condition to promote the stem cell state (**Okae et al. 2018; Varberg et al. 2023**). CYP1A1 and CYP1B1 increased dramatically in response to TCDD exposure (**Figure 1A-C**). Exposure of TS cells maintained in the stem state to TCDD (10 nM) did not adversely affect cell viability or cell cycle (**Figure S1**). Analysis of RNA-seq of TCDD treated versus control cells resulted in the identification of 668 differentially expressed genes (**DEGs**), including 484 genes upregulated and 184 genes downregulated by exposure to TCDD (10 nM) (**Figure 1D and Dataset 1**). This differential gene expression pattern was validated by RT-qPCR (**Figure 1E and F**). Functional pathways affected by TCDD exposure, included pathways associated with protein translation and cell-extracellular matrix adhesion (**Figure S2**). We also examined the consequences of human TS cell TCDD exposure (10 or 25 nM) during the stem state (24 h) on subsequent EVT cell and ST

differentiation. TCDD exposure during the stem state did not adversely affect EVT cell or ST differentiation (**Figure S3**).

EVT cell differentiation state. TCDD exposure did not adversely affect the morphology of differentiated EVT cells (**Figure 2A**); however, TCDD exposure did increase CYP1A1 and CYP1B1 transcript levels and CYP1A1 protein expression (**Figure 2B and C**). RNA-seq analysis of control and TCDD exposed cells identified 336 DEGs, including 173 upregulated transcripts and 163 downregulated transcripts in TCDD treated cells (**Dataset 2, Figure 2D**). RT-qPCR validation of a subset of these transcripts is shown (**Figure 2E and F**). Functional pathways affected by TCDD exposure, included pathways associated with protein translation, cell-cell interactions, and cell death (**Figure S4**).

ST differentiation state. TCDD exposure did not adversely affect the morphology of differentiated ST (**Figure 3A**); however, TCDD exposure during ST differentiation did increase the expression of *CYP1A1* and *CYP1B1* (**Figure 3B**). RNA-seq analysis of control and TCDD exposed cells identified 353 DEGs, including 154 upregulated genes and 199 downregulated genes in TCDD treated cells (**Dataset 3, Figure 3C**). RT-qPCR validation of a subset of these transcripts is shown (**Figure 3D**). Functional pathways affected by TCDD exposure, included pathways associated with estrogen biosynthesis and AHR and hypoxia signaling (**Figure S5**).

Cells in each trophoblast cell differentiation state exhibited similar TCDD induced activation of CYP1A1 and CYP1B1 (**Figures 1-3**). However, based on the total number of DEGs, TS cells in the stem state were maximally responsive to TCDD (668 DEGs), whereas EVT cells were the least responsive to TCDD (336 DEGs). ST exhibited an intermediate response to TCDD (353 DEGs). These observations indicate that TS cells in the stem state may be more vulnerable to TCDD exposure than differentiated trophoblast cells.

Role of AHR in TCDD induction of CYP1A1 and CYP1B1

We next tested whether TCDD effects on *CYP1A1* and *CYP1B1* expression in human TS cells were dependent upon AHR using a loss-of-function approach. AHR expression was silenced in human TS cells using stable lentiviral-mediated delivery of control and AHR-targeted shRNAs. Disruption of AHR expression was verified by RT-qPCR, western blotting, and immunofluorescence (**Figure 4A-C**). AHR knockdown TS cells maintained in the stem state did not effectively respond to TCDD with an induction of *CYP1A1* and *CYP1B1* expression (**Figure 4D**). The results demonstrated that TCDD induction of *CYP1A1* and *CYP1B1* gene expression is AHR dependent.

TCDD driven 2ME biosynthesis in human TS cells

In the above experimentation, we observed significant effects of TCDD exposure on gene expression but not on the maintenance of the human TS cell stem state or in the capacity for human TS cells to differentiate into EVT cells or ST. CYP1A1 expression was especially

responsive to TCDD and has the capacity to transform endogenous and exogenous compounds, including 17β estradiol, into biologically active molecules such as 2ME (**Thomas and Potter 2013**). Consequently, we examined the effects of TCDD on the capacity of human TS cells in the presence of 17β estradiol to synthesize 2ME. TCDD exposure significantly stimulated 2ME biosynthesis in human TS cells maintained in the stem cell state (**Figure 5A**) and TS cells induced to differentiate into EVT cells or ST (**Figure 5B**).

A pathway showing the involvement of AHR, CYP1A1, and 2ME in xenobiotic action at the placentation site is shown (**Figure 5C**).

DISCUSSION

The placenta serves as the interface between maternal and fetal compartments. Trophoblast cells are specialized cells of the placenta with the capacity to respond to internal and external signals and can act to modify maternal and fetal environments. In this report, we discovered that TCDD activates AHR signaling in human trophoblast cells and evokes a robust transcriptional response, which includes stimulating CYP1A1 expression. Human trophoblast cells have similarly been shown to respond to AHR ligands with an increase in CYP1A1 gene expression (**Stejskalova et al. 2011; Wakx et al. 2018).** These TCDD activated changes in cell behavior do not adversely affect the ability of human TS cells to self-renew or to differentiate into either EVT cells or ST. However, they can affect the availability of biologically active ligands at the maternal-fetal interface.

TCDD does not adversely affect the development of rat or human trophoblast cells (**Iqbal et al. 2021; present study**). Rat trophoblast cells lack the requisite cellular machinery needed to respond to TCDD, while human trophoblast cells are responsive to TCDD, but without negative consequences on TS cell self-renewal, maintenance of the TS cell stem state or the differentiation of TS cells into EVT cells and ST. This is an adaptive characteristic of placentation in the rat and human. The environment is replete with compounds possessing the capacity to activate AHR signaling (**Birnbaum 1994; DeGroot et al. 2012; Murray and Perdue 2020**). Thus, an adverse effect of AHR signaling on placental morphogenesis would be problematic. Retention of the capacity for placental morphogenesis and establishment of placental structure and function to combat the adverse effects of an environmental toxicant represents a strategy for maximizing survival of fetus.

The relevance of species differences in trophoblast cell engagement with its environment is unknown. At one level, survival of a species would appear to be enhanced by the ability to actively adapt to the environment, especially through the upregulation of an enzyme that can transform a potentially dangerous compound into a compound that can be made less threatening or extricated from the body. This implies that the actions of environmentally activated enzymes possessing biotransformational properties are unilateral in their efforts. This is not the case for AHR and its downstream targets, especially CYP1A1. Endogenous AHR ligands are present in the cellular milieu (**Nguyen and Bradfield, 2008**) and CYP1A1 can act on endogenous compounds (**Stejskalova and Pavek, 2011; Bock 2014**). Among the endogenous compounds that CYP1A1 can act on is the steroid hormone, 17β estradiol (**Thomas and Potter 2013**). Biosynthesis of estrogens represents a key species difference in the evolution of the placenta

(**Soares et al. 2018**). Trophoblast cells of the human placenta possess aromatase (cytochrome P450 family 19 subfamily A member 1, CYP19A1), the enzyme responsible for conversion of androgens to estrogens (**Albrecht and Pepe 1990; Simpson et al. 1997**), whereas this key enzyme in estrogen biosynthesis is not present in placentas of the rat and mouse (**Kamat et al. 2002**). Interestingly, estrogen action and AHR signaling have been linked (**Tarnow et al. 2019**). Thus, species differences in trophoblast cell responses to environmental signals capable of activating AHR signaling may be linked to species differences in placental capacity for estrogen biosynthesis. Investigating the relationship of AHR signaling and estrogen biosynthesis in placentas of other species could be informative.

The most prominent effect of TCDD on human trophoblast cells was on the expression of CYP1A1. CYP1A1 does little to affect cell function unless there is a substrate for it to act on. As indicated above, 17β estradiol is a notable CYP1A1 substrate produced within the human placenta. Estrogens are prominent activators of two nuclear estrogen receptors (**Deroo and Korach 2006**), which are critical for reproductive function, including the establishment and maintenance of pregnancy (**Deroo and Korach 2006; Hewitt et al. 2016**). CYP1A1 can hydroxylate estradiol to 2-hydroxyestradiol and 4-hydroxyestradiol (catechol estrogens) (**Thomas and Potter 2013; Kumar et al. 2016**). These modifications of estradiol decrease its availability for signaling through nuclear estrogen receptors and generate biologically active compounds with different properties. Catechol-O-methyltransferase (**COMT**) can modify 2-hydroxyestradiol to 2ME (**Thomas and Potter 2013; Kumar et al. 2016**). Human trophoblast cells exposed to TCDD exhibit an enhanced capacity to convert estradiol to 2ME (**present study**). 2ME is a compound with biological functions implicated in regulatory processes

associated with angiogenesis, cellular responses to hypoxia, and preeclampsia (**Mabjeesh et al. 2003; Kanasaki et al. 2008; Lee et al. 2010; Perez-Sepulveda et al. 2013; Pinto et al. 2014**).

Collectively, these findings indicate that TCDD, a prototypical AHR ligand, has the capacity to influence the behavior of trophoblast cells within the human maternal-fetal interface and potentially pregnancy outcomes.

ACKNOWLEDGMENTS

We thank Stacy Oxley, Leslie Tracy, and Brandi Miller for their assistance. Research was supported by KUMC BRTP and K-INBRE P20 GM103418 (VS), National Institutes of Health: ES028957 (KI) and HD020676, ES029280, HD105734 and the Sosland Foundation.

DATA SHARING

The datasets generated and analyzed for this study have been deposited in the Gene Expression Omnibus (**GEO**) database, https://www.ncbi.nlm.nih.gov/geo/ (accession no. GSE246513).

REFERENCES

Albrecht ED, Pepe GJ. 1990. Placental steroid hormone biosynthesis in primate pregnancy. Endocr Rev 11(1):124-150.

Asanoma K, Rumi MA, Kent LN, Chakraborty D, Renaud SJ, Wake N, Lee DS, Kubota K, Soares MJ. 2011. FGF4-dependent stem cells derived from rat blastocysts differentiate along the trophoblast lineage. Dev Biol 351(1):110-119.

Avilla MN, Malecki KM, Hahn ME, Wilson RH, Bradfield CA. 2020. The Ah receptor: Adaptive metabolism, ligand diversity, and the xenokine model. Chem Res Toxicol 33(4):860-879.

Barouki R, Gluckman PD, Grandjean P, Hanson M, Heindel JJ. 2012. Developmental origins of non-communicable disease: implications for research and public health. Environ Health 11:42.

Beischlag TV, Luis Morales J, Hollingshead BD, Perdew GH. 2008. The aryl hydrocarbon receptor complex and the control of gene expression. Crit Rev Eukaryot Gene Expr 18(3):207-250.

Bock KW. 2014. Homeostatic control of xeno- and endobiotics in the drug-metabolizing enzyme system. Biochem Pharmacol 90:1-6.

Burton GJ, Fowden AL, Thornburg KL. 2016. Placental origins of chronic disease. Physiol Rev 96(4):1509-1565.

Casado FL, Singh KP, Gasiewicz TA. 2010. The aryl hydrocarbon receptor: regulation of hematopoiesis and involvement in the progression of blood diseases. Blood Cells Mol Dis 44(4):199-206.

Deroo BJ, Korach KS. 2006. Estrogen receptors and human disease. J Clin Invest 116:561-570.

Drukteinis J, Medrano T, Ablordeppey EA, Kitzman JM, Shiverick KT. 2005. Benzo[a]pyrene, but not 2,3,7,8-TCDD, induces G2/M cell cycle arrest, p21CIP1 and p53 phosphorylation in human choriocarcinoma JEG-3 cells: a distinct signaling pathway. Placenta 26:S87-S95.

Drwal E, Rak A, Gregoraszczuk EL. 2019. Differential effects of ambient PAH mixtures on cellular and steroidogenic properties of placental JEG-3 and BeWo cells. Reprod Toxicol 86:14-22.

Fadiel A, Epperson B, Shaw MI, Hamza A, Petito J, Naftolin F. 2013. Bioinformatic analysis of benzo-α-pyrene-induced damage to the human placental insulin-like growth factor-1 gene. Reprod Sci 20(8):917-928.

Guyda HJ, Mathieu L, Lai W, Manchester D, Wang SL, Ogilvie S, Shiverick KT. 1990. Benzo(a)pyrene inhibits epidermal growth factor binding and receptor autophosphorylation in human placental cell cultures. Mol Pharmacology 37(2):137-143.

Hewitt SC, Winuthayanon W, Korach KS. 2016. What's new in estrogen receptor action in the female reproductive tract. J Mol Endocrinol 56:R55-R71.

Iqbal K, Pierce SH, Kozai K, Dhakal P, Scott RL, Roby KF, Vyhlidal CA, Soares MJ. 2021. Evaluation of placentation and the role of the aryl hydrocarbon receptor pathway in a rat model of dioxin exposure. Environ Health Perspect 129(11):117001.

Kamat A, Hinshelwood MM, Murry BA, Mendelson CR. 2002. Mechanisms in tissue-specific regulation of estrogen biosynthesis in humans. Trends Endocrinol Metab 13(3):122-128.

Kanasaki K, Palmsten K, Sugimoto H, Ahmad S, Hamano Y, Xie L, Parry S, Augustin HG, Gattone VH, Folkman J, Strauss JF, Kalluri R. 2008. Deficiency in catechol-O-methyltransferase and 2-methoxyestradiol is associated with pre-eclampsia. Nature 453:1117-1121.

Knöfler M, Haider S, Saleh L, Pollheimer J, Gamage TKJB, James J. 2019. Human placenta and trophoblast development: key molecular mechanisms and model systems. Cell Mol Life Sci 76(18):3479-3496.

Kumar BS, Raghuvanshi DS, Hasanain M, Alam S, Sardar J, Mitra K, Khan F, Negi AS. 2016. Recent advances in chemistry and pharmacology of 2-methoxyestradiol: an anticancer investigational drug. Steroids 110:9-34.

Lee CQ, Gardner L, Turco M, Zhao N, Murray MJ, Coleman N, Rossant J, Hemberger M, Moffett A. 2016. What is trophoblast? A combination of criteria define human first-trimester trophoblast. Stem Cell Reports 6(2):257-272.

Lee SB, Wong AP, Kansasaki K, Xu Y, Shenoy VK, McElrath TF, Whitesides GM, Kalluri R. 2010. Preeclampsia: 2-methoxyestradiol induces cytotrophoblast invasion and vascular development specifically under hypoxic conditions. Am J Pathol 176:710-720.

Le Vee M, Kolasa E, Jouan E, Collet N, Fardel O. 2014. Differentiation of human placental BeWo cells by the environmental contaminant benzo(a)pyrene. Chem Biol Interact 210:1-11.

Liu G, Jia J, Zhong J, Yang Y, Bao Y, Zhu Q. 2022. TCDD-induced IL-24 secretion in human chorionic stromal cells inhibits placental trophoblast cell migration and invasion. Reprod Toxicol 108:10-17.

Ma Q. 2001. Induction of CYP1A1. The AhR/DRE paradigm: transcription, receptor regulation, and expanding biological roles. Curr Drug Metab 2(2):149-164.

Mabjeesh NJ, Escuin D, LaVallee TM, Pribluda VS, Swartz GM, Johnson MS, Willard MT, Zhong H, Simons JW, Giannakakou P. 2003. 2ME2 inhibits tumor growth and angiogenesis by disrupting microtubules and dysregulating HIF. Cancer Cell 3:363-375.

Marsit CJ. 2016. Placental epigenetics in children's environmental health. Semin Reprod Med 34(1):36-41.

Matsumoto S, Porter CJ, Ogasawara N, Iwatani C, Tsuchiya H, Seita Y, Chang YW, Okamoto I, Saitou M, Ema M, Perkins TJ, Stanford WL, Tanaka S. 2020. Establishment of macaque trophoblast stem cell lines derived from cynomolgus monkey blastocysts. Sci Rep 10(1):6827.

Mattison DR. 2010. Environmental exposures and development. Curr Opin Pediatr 22(2):208-218.

McIntosh BE, Hogenesch JB, Bradfield CA. 2010. Mammalian Per-Arnt-Sim proteins in environmental adaptation. Annu Rev Physiol 72(1):625-645.

Murray IA, Perdew GH. 2020. How Ah receptor ligand specificity became important in understanding its physiological function. Int J Mol Sci 21(24):9614.

Nguyen LP, Bradfield CA. 2008. The search for endogenous activators of the aryl hydrocarbon receptor. Chem Res Toxicol 21(1):102-116.

Okae H, Toh H, Sato T, Hiura H, Takahashi S, Shirane K, Kabayama Y, Suyama M, Sasaki H, Arima T. 2018. Derivation of human trophoblast stem cells. Cell Stem Cell 22(1):50-63.e6.

Perez-Sepulveda A, Espana-Perrot PP, Norwitz ER, Illanes SE. 2013. Metabolic pathways involved in 2-methoxyestradiol synthesis and their role in preeclampsia. Reprod Sci 20:1020-1029.

Pinto MP, Medina RA, Owen GI. 2014. 2-Methoxyestradiol and disorders of female reproductive tissues. Horm Canc 5:274-283.

Schmidt JK, Keding LT, Block LN, Wiepz GJ, Koenig MR, Meyer MG, Dusek BM, Kroner KM, Bertogliat MJ, Kallio AR, Mean KD, Golos TG. 2020. Placenta-derived macaque trophoblast stem cells: differentiation to syncytiotrophoblasts and extravillous trophoblasts reveals phenotypic reprogramming. Sci Rep 10(1):19159.

Shukla V, Soares MJ. 2022. Modeling trophoblast cell-guided uterine spiral artery transformation in the rat. Int J Mol Sci 23(6):2947.

Simpson ER, Zhao Y, Agarwal VR, Michael MD, Bulun SE, Hinshelwood MM, Graham-Lorence S, Sun T, Fisher CR, Qin K, Mendelson CR. 1997. Aromatase expression in health and disease. Recent Prog Horm Res 52:185-213.

Soares MJ, Varberg KM, Iqbal K. 2018. Hemochorial placentation: development, function, and adaptations. Biol Reprod 99(1):196-211.

Stejskalova L, Pavek P. 2011. The function of cytochrome P450 1A1 enzyme (CYP1A1) and aryl hydrocarbon receptor (AhR) in the placenta. Curr Pharmaceut Biotechnol 12:715-730.

Stejskalova L, Rulcova A, Vrzal R, Dvorak Z, Pavek P. 2013. Dexamethasone accelerates degradation of aryl hydrocarbon receptor (AHR) and suppresses CYP1A1 induction in placental JEG-3 cell line. Toxicol Lett 223(2):183-191.

Stejskalova L, Vecerova L, Peréz LM, Vrzal R, Dvorak Z, Nachtigal P, Pavek P. 2011. Aryl hydrocarbon receptor and aryl hydrocarbon nuclear translocator expression in human and rat placentas and transcription activity in human trophoblast cultures. Toxicol Sci 123(1):26-36.

Tanaka S, Kunath T, Hadjantonakis AK, Nagy A, Rossant J. 1998. Promotion of trophoblast stem cell proliferation by FGF4. Science 282(5396):2072-2075.

Tarnow P, Tralau T, Luch A. 2019. Chemical activation of estrogen and aryl hydrocarbon receptor signaling pathways and their interaction in toxicology and metabolism. Expert Opin Drug Metab Toxicol 15(3):219-229.

Thomas MP, Potter BVL. 2013. The structural biology of oestrogen metabolism. J Steroid Biochem Mol Biol 137:27-49.

Tsang H, Cheung TY, Kodithuwakku SP, Chai J, Yeung WS, Wong CK, Lee KF. 2012. 2,3,7,8-Tetrachlorodibenzo-p-dioxin (TCDD) suppresses spheroids attachment on endometrial epithelial cells through the down-regulation of the Wnt-signaling pathway. Reprod Toxicol 33(1):60-66.

Varberg KM, Dominguez EM, Koseva B, Varberg JM, McNally RP, Moreno-Irusta A, Wesley ER, Iqbal K, Cheung WA, Schwendinger-Schreck C, Smail C, Okae H, Arima T, Lydic M, Holoch K, Marsh C, Soares MJ, Grundberg E. 2023. Extravillous trophoblast cell lineage development is associated with active remodeling of the chromatin landscape. Nat Commun 14(1):4826.

Vazquez-Rivera E, Rojas B, Parrott JC, Shen AL, Xing Y, Carney PR, Bradfield CA. 2021. The aryl hydrocarbon receptor as a model PAS sensor. Toxicol Rep 9:1-11.

Vrooman LA, Xin F, Bartolomei MS. 2016. Morphologic and molecular changes in the placenta: what we can learn from environmental exposures. Fertil Steril 106(4):930-940.

Wakx A, Nedder M, Tomkiewicz-Raulet C, Dalmasso J, Chissey A, Boland S, Vibert F, Degrelle SA, Fournier T, Coumoul X, Gil S, Ferecatu I. 2018. Expression, localization, and activity of the aryl hydrocarbon receptor in the human placenta. Int J Mol Sci 19(12):3762.

Wesselink A, Warner M, Samuels S, Parigi A, Brambilla P, Mocarelli P, Eskenazi B. 2014. Maternal dioxin exposure and pregnancy outcomes over 30 years of follow-up in Seveso. Environ Int 63:143-148.

Whitlock JP Jr. 1999. Induction of cytochrome P4501A1. Annu Rev Pharmacol Toxicol 39:103-125.

Wright EJ, De Castro KP, Joshi AD, Elferink CJ. 2017. Canonical and non-canonical aryl hydrocarbon receptor signaling pathways. Curr Opin Toxicol 2:87-92.

Ye Y, Jiang S, Du T, Ding M, Hou M, Mi C, Liang T, Zhong H, Xie J, Xu W, Zhang H. 2021. Environmental pollutant benzo[a]pyrene upregulated long non-coding RNA Hz07 inhibits trophoblast cell migration by inactivating PI3K/AKT/MMP2 signaling pathway in recurrent pregnancy loss. Reprod Sci 28(11):3085-3093.

Zablon HA, Ko CI, Puga A. 2021. Converging roles of the aryl hydrocarbon receptor in early embryonic development, maintenance of stemness, and tissue repair. Toxicol Sci 182(1):1-9.

Zhang L, Connor EE, Chegini N, Shiverick KT. 1995. Modulation by benzo[a]pyrene of epidermal growth factor receptors, cell proliferation, and secretion of human chorionic gonadotropin in human placental cell lines. Biochem Pharmacol 50(8):1171-1180.

Zhang L, Shiverick KT. 1997. Benzo(a)pyrene, but not 2,3,7,8-tetrachlorodibenzo-p-dioxin, alters cell proliferation and c-myc and growth factor expression in human placental choriocarcinoma JEG-3 cells. Biochem Biophys Res Commun 231(1):117-120.

Zhang L, Shiverick KT. 1998. Differential effects of 2,3,7,8-tetrachlorodibenzo-p-dioxin and benzo(a)pyrene on proliferation and growth factor gene expression in human choriocarcinoma BeWo cells. Placenta 19:177-191.

Zhou Y, Zhou B, Pache L, Chang M, Khodabakhshi AH, Tanaseichuk O, Benner C, Chanda SK. 2019. Metascape provides a biologist-oriented resource for the analysis of systems-level datasets. Nat Commun 10(1):1523.

FIGURE LEGENDS

Figure 1. Effects of TCDD on human TS cells in the stem state. (A, B) *CYP1A1* and *CYP1B1* transcript levels in human TS cells exposed to Control conditions or TCDD (1-100 nM) for 24 h. (C) Immunocytochemistry of CYP1A1 protein expression in human TS cells exposed to Control conditions or TCDD (10 nM) for 24 h (Scale bar: 300 μm). DAPI identifies cell nuclei (blue). (D) Heatmap showing select transcripts from RNA-seq analysis of human TS cells exposed to Control conditions or TCDD (10 nM) 24 h. (E, F) RT-qPCR validation of selected up regulated and down-regulated transcripts in human TS cells exposed to Control or TCDD (10 nM). n=3. Graphs represent mean values ± standard error of the mean (**SEM**), unpaired t test, *P < 0.05, **P < 0.01, and ***P < 0.001.

Figure 2. Effect of TCDD in EVT cells. (A) Phase-contrast images depicting cell morphology of EVT cells differentiated from human TS cells in presence of vehicle or TCDD (10 nM) (Scale bar = 500 μm). (B) Expression of CYP1A1 and CYP1B1 following exposure to vehicle or TCDD (10 nM) during EVT cell differentiation. (C) Immunofluorescence of CYP1A1 expression (red) in EVT cells treated with vehicle and TCDD (10 nM) (Scale bar: 300 μm). DAPI marks cell nuclei (blue). (D) Heatmap showing select transcripts from RNA-seq analysis of EVT cells exposed to vehicle versus TCDD (10 nM). (E, F) RT-qPCR validation of selected up-regulated and down-regulated transcripts in vehicle versus TCDD treated cells. n = 3. Graphs represent mean values ± SEM, unpaired t test, *P < 0.05, **P < 0.01, and ***P < 0.001.

Figure 3. Effect of TCDD in syncytiotrophoblast differentiation. (A) Phase-contrast images depicting three-dimensional (**3D**) syncytiotrophoblast development in presence of vehicle or TCDD (10 nM) (Scale bar = 300 μm). (B) Expression of CYP1A1 and CYP1B1 following exposure to vehicle or TCDD (10 nM) during 2D and 3D syncytiotrophoblast

differentiation. (C) Heatmap showing select transcripts from RNA-seq analysis of 3D syncytiotrophoblast exposed to vehicle versus TCDD (10 nM). (D) RT-qPCR validation of selected up-regulated transcripts in cells treated with vehicle versus TCDD, n=3. Graphs represent mean values ± SEM, unpaired t test, *P < 0.05, **P < 0.01, and ***P < 0.001.

Figure 4. AHR dependent activation of CYP1A1 in human TS cells. RT-qPCR (A) and western blot (B) assessment of lentiviral vector-mediated AHR silencing efficiency in human TS cells expressing control or AHR shRNAs. (C) Immunocytochemistry of AHR protein expression (green) in control shRNA or AHR shRNA silenced cells (Scale bar: 300μm). DAPI marks cell nuclei (blue). (D) CYP1A1 and CYP1B1 transcript level measurements in control shRNA or AHR shRNA silenced cells in presence of TCDD (10 nM) for 24 h. n=3. Graphs represent mean values ± SEM, one-way ANOVA analysis, Tukey's post hoc test. *P < 0.05, **P < 0.01, ***P < 0.001, ****P < 0.0001.

Figure 5. Effects of TCDD on 2-methoxyestradiol production by human TS cells. 2-methoxyestradiol concentration (pmole/mL) measured in TS cells maintained in the stem state (A) or induced to differentiate into EVT cells or ST (B). Cells were exposed to vehicle + estradiol (E2; 10 nM) or TCDD (10 nM) + E2 (10 nM) for 48 h before harvesting conditioned medium for 2-methoxyestradiol measurement. n=3. Graphs represent mean values ± SEM, unpaired t test, *P < 0.05, and **P < 0.01 (C) Schematic of a TCDD-mediated pathway affecting placentation.

SUPPLEMENTARY FIGURES

Figure S1. Effects of TCDD on human cell cycle and cell death. (A) Human TS cells were stained with annexin-V (**AV**) and propidium iodide (**PI**) and subjected to flow cytometry to determine cell death. Human TS cells were treated with vehicle or TCDD (10 and 100 nM). (B) Human TS cells were stained with PI and subjected to flow cytometry to determine DNA content and stage of the cell cycle.

Figure S2. Pathway analysis of RNA-sequencing datasets of human TS cells maintained in the stem state exposed to vehicle or TCDD (10 nM).

Figure S3. Effects of TCDD exposure in the stem state on the capacity of human TS cells to differentiate. Human TS cells were treated in the stem state with TCDD (10 nM) for 24 h and then induced to differentiate into EVT cells or ST. (A) Morphology of human TS cells induced to differentiated into EVT cells. (B) RT-qPCR measurement of *HLA-G* and *MMP2* levels, transcripts associated with EVT cell differentiation. (C) Morphology of human TS cells induced to differentiated into ST. (D) RT-qPCR measurement of *CGB5* and *SDC1* levels, transcripts associated with ST differentiation.

Figure S4. Pathway analysis of RNA-sequencing datasets of human TS cells induced to differentiate into EVT cells exposed to vehicle or TCDD (10 nM).

Figure S5. Pathway analysis of RNA-sequencing datasets of human TS cells induced to differentiate into ST exposed to vehicle or TCDD (10 nM).

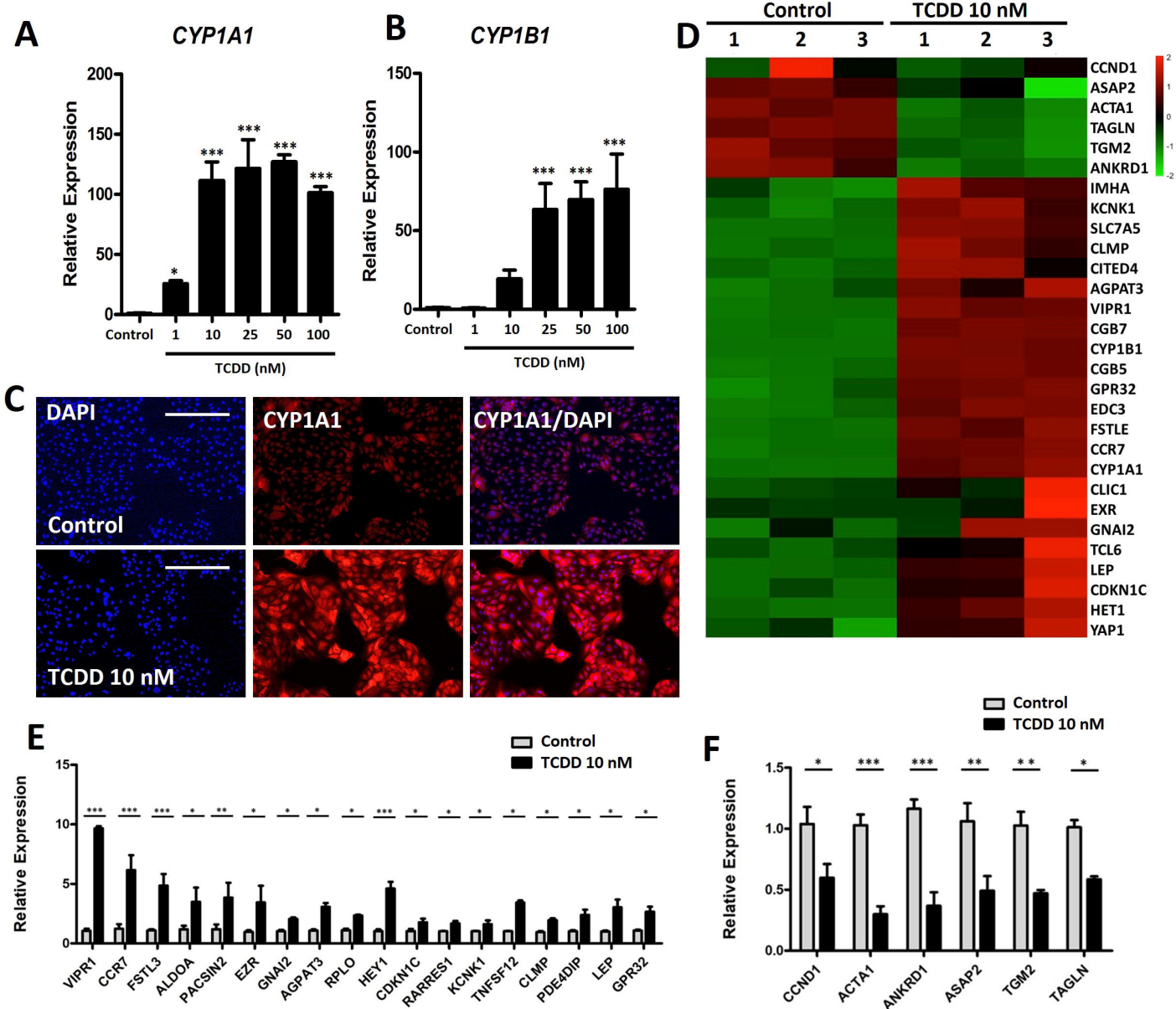
A
CYP1A1
Relative Expression
200
150
100
50
0
Control
1
10
25
50
100
TCDD (nM)
B
CYP1B1
Relative Expression
150
100
50
0
Control
1
10
25
50
100
TCDD (nM)
C
DAPI
CYP1A1
CYP1A1/DAPI
Control
TCDD 10 nM
D
Control
TCDD 10 nM
1
2
3
1
2
3
CCND1
ASAP2
ACTA1
TAGLN
TGM2
ANKRD1
IMHA
KCNK1
SLC7A5
CLMP
CITED4
AGPAT3
VIPR1
CGB7
CYP1B1
CGB5
GPR32
EDC3
FSTLE
CCR7
CYP1A1
CLIC1
EXR
GNAI2
TCL6
LEP
CDKN1C
HET1
YAP1
E
Control
TCDD 10 nM
Relative Expression
VIPR1
CCR7
FSTL3
ALDOA
PACSIN2
EZR
GNAI2
AGPAT3
RPLO
HEY1
CDKN1C
RARRES1
KCNK1
TNFSF12
CLMP
PDE4DIP
LEP
GPR32
F
Control
TCDD 10 nM
Relative Expression
CCND1
ACTA1
ANKRD1
ASAP2
TGM2
TAGLN

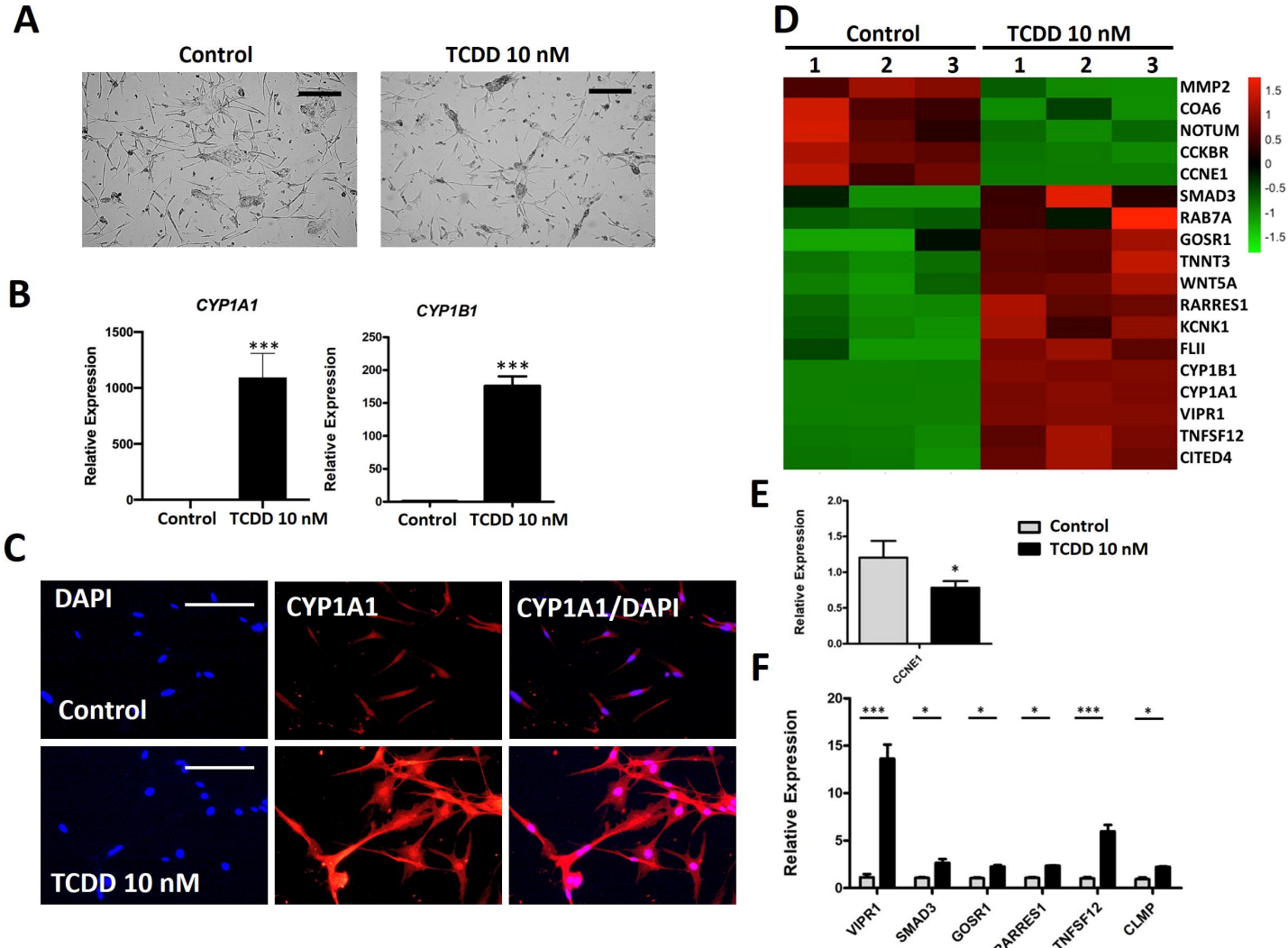
A
Control
TCDD 10 nM
B
CYP1A1
CYP1B1
Relative Expression
1500
1000
500
0
250
200
150
100
50
***
Control
TCDD 10 nM
C
DAPI
CYP1A1
CYP1A1/DAPI
Control
TCDD 10 nM
D
Control
TCDD 10 nM
1
2
3
MMP2
COA6
NOTUM
CCKBR
CCNE1
SMAD3
RAB7A
GOSR1
TNNT3
WNT5A
RARRES1
KCNK1
FLII
CYP1B1
CYP1A1
VIPR1
TNFSF12
CITED4
1.5
1
0.5
0
-0.5
-1
-1.5
E
Relative Expression
2.0
1.5
1.0
0.5
0.0
*
CCNE1
Control
TCDD 10 nM
F
Relative Expression
20
15
10
5
0
***
*
VIPR1
SMAD3
GOSR1
RARRES1
TNFSF12
CLMP

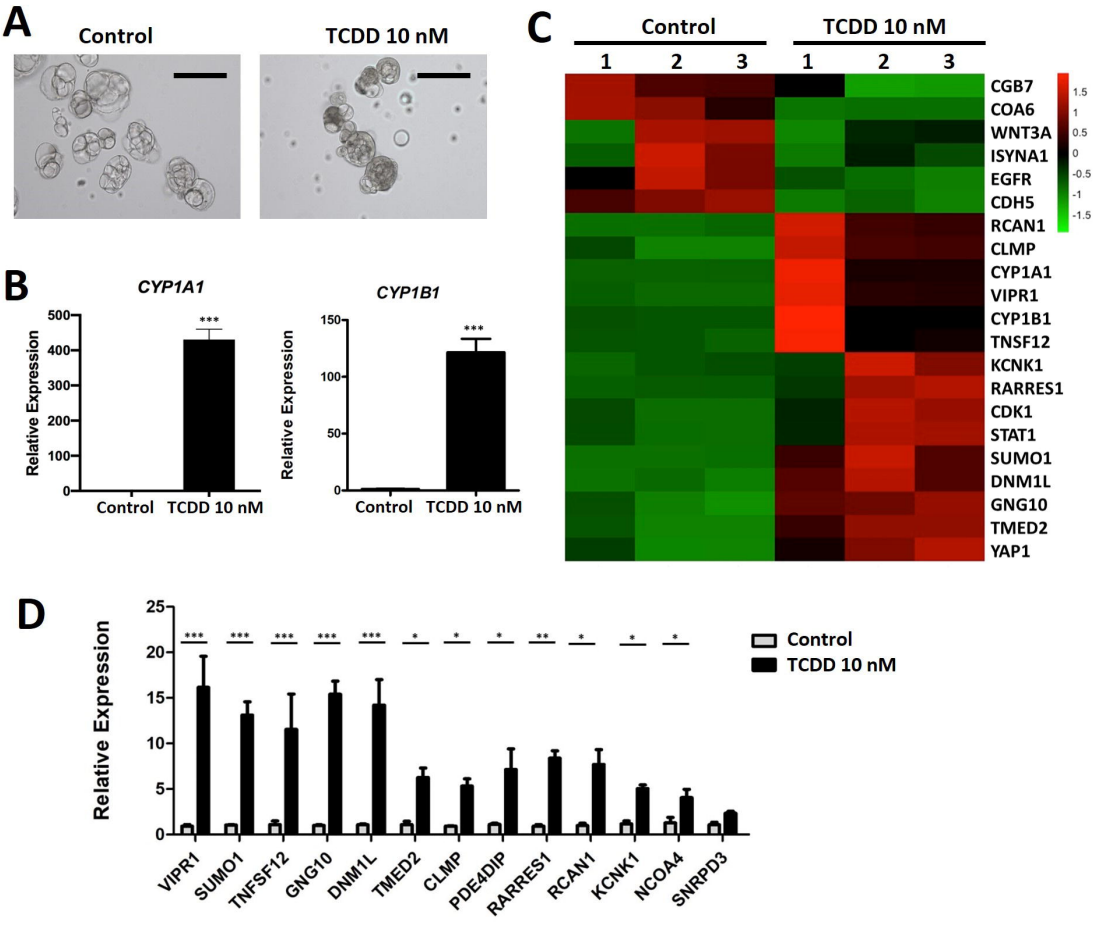
A
Control
TCDD 10 nM
B
CYP1A1
CYP1B1
Relative Expression
Control
TCDD 10 nM
C
Control
TCDD 10 nM
1 2 3 1 2 3
CGB7
COA6
WNT3A
ISYNA1
EGFR
CDH5
RCAN1
CLMP
CYP1A1
VIPR1
CYP1B1
TNSF12
KCNK1
RARRES1
CDK1
STAT1
SUMO1
DNM1L
GNG10
TMED2
YAP1
D
Relative Expression
Control
TCDD 10 nM
VIPR1
SUMO1
TNFSF12
GNG10
DNM1L
TMED2
CLMP
PDE4DIP
RARRES1
RCAN1
KCNK1
NCOA4
SNRPD3

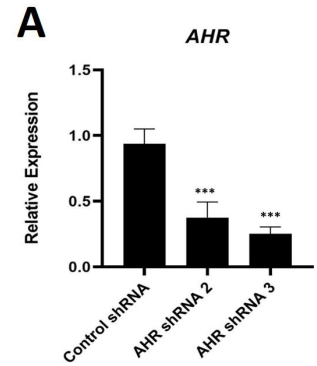
A
AHR
Relative Expression
1.5
1.0
0.5
0.0
***
***
Control shRNA
AHR shRNA 2
AHR shRNA 3

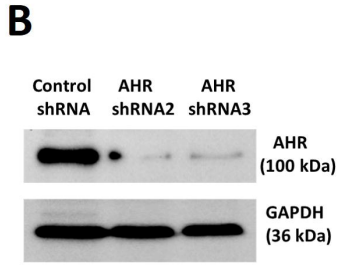
B
Control shRNA
AHR shRNA2
AHR shRNA3
AHR (100 kDa)
GAPDH (36 kDa)

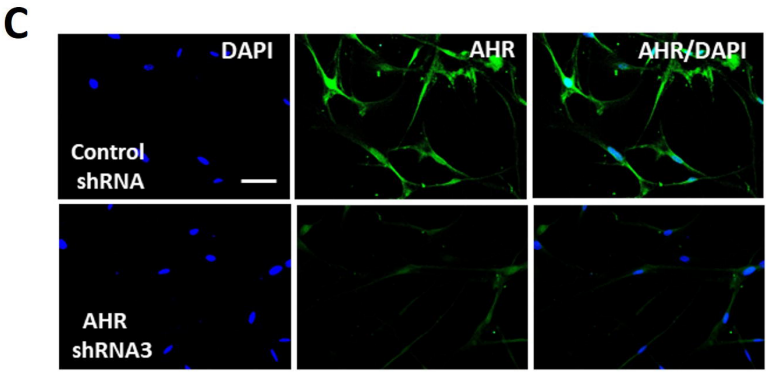
C
DAPI
AHR
AHR/DAPI
Control shRNA
AHR shRNA3

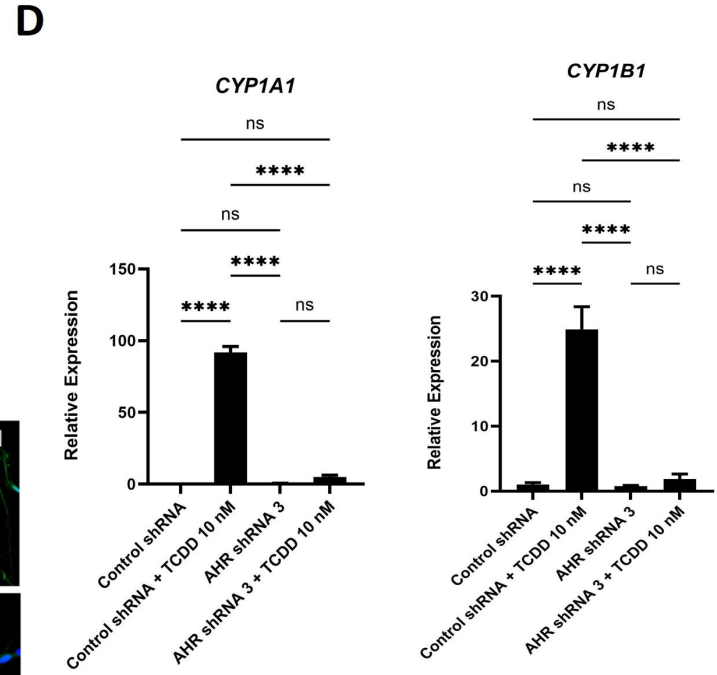
D
CYP1A1
Relative Expression
150
100
50
0
ns
****
ns
****
****
ns
Control shRNA
Control shRNA + TCDD 10 nM
AHR shRNA 3
AHR shRNA 3 + TCDD 10 nM
CYP1B1
Relative Expression
30
20
10
0
ns
****
ns
****
****
ns
Control shRNA
Control shRNA + TCDD 10 nM
AHR shRNA 3
AHR shRNA 3 + TCDD 10 nM

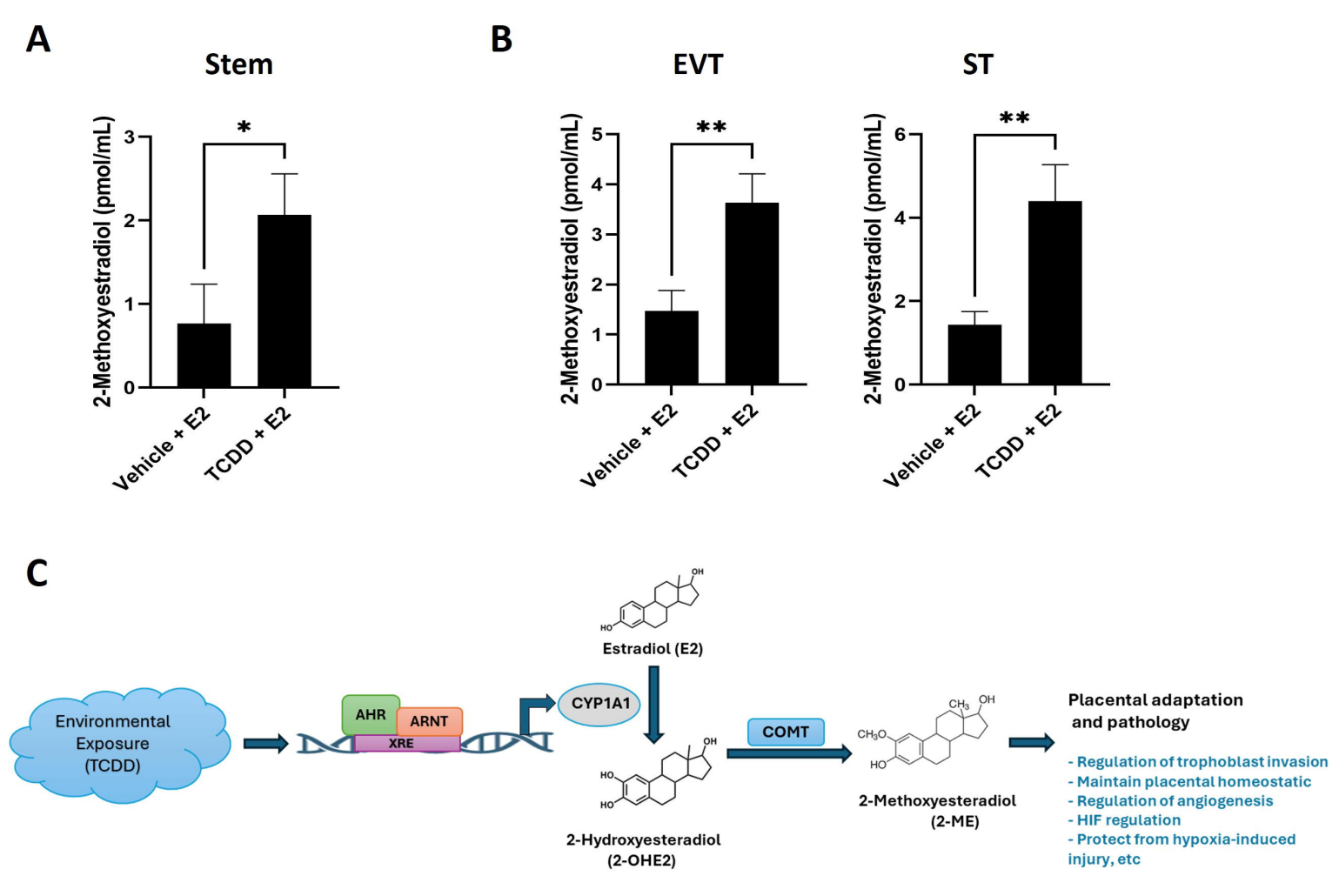
A
Stem
2-Methoxyestradiol (pmol/mL)
0
1
2
3
*
Vehicle + E2
TCDD + E2
B
EVT
2-Methoxyestradiol (pmol/mL)
0
1
2
3
4
5
**
Vehicle + E2
TCDD + E2
ST
2-Methoxyestradiol (pmol/mL)
0
2
4
6
**
Vehicle + E2
TCDD + E2
C
Environmental Exposure (TCDD)
AHR
ARNT
XRE
CYP1A1
Estradiol (E2)
2-Hydroxyesteradiol (2-OHE2)
COMT
2-Methoxyesteradiol (2-ME)
Placental adaptation and pathology
- Regulation of trophoblast invasion
- Maintain placental homeostatic
- Regulation of angiogenesis
- HIF regulation
- Protect from hypoxia-induced injury, etc